Journal of Applied Electrochemistry (2019) 49:87–97
https://doi.org/10.1007/s10800-018-1273-4

RESEARCH ARTICLE

Implementation of electrochemical impedance spectroscopy to evaluate HER-2 aptamer conjugation to Ecoflex® nanoparticles for docetaxel delivery in breast cancer cells

Jaleh Varshosaz[1,5] · Erfaneh Ghassami[1] · Abdollah Noorbakhsh[2] · Ali Jahanian-Najafabadi[3] · Mohsen Minayian[4]

Received: 9 July 2018 / Accepted: 9 November 2018 / Published online: 19 November 2018

Abstract

Aptamers are affinity molecules with high specificity, proposed as excellent alternatives to antibodies in targeting and detecting applications due to their smaller size, higher stability, and simplicity of production and modification compared with antibodies. Due to lack of a sensitive and simple method to quantitatively evaluate attachment of aptamer to nanoparticles (NPs), optimization of the attachment process was not considered in most of previously studied aptamer-targeted drug delivery systems. The aim of current study was to demonstrate the utility of electrochemical impedance spectroscopy (EIS) technique in this field. Ecoflex® polymeric NPs loaded with docetaxel (DTX-NPs) were fabricated via electrospraying technique, and HER-2-specific aptamer molecules were attached via amide bonds (Apt-DTX-NPs). Using EIS method, the time period of various stages of aptamer conjugation was optimized, by comparing the amount of aptamer molecules attached to the DTX-NPs. The results of in vitro studies on optimum Apt-DTX-NPs demonstrated that the proposed delivery system could significantly enhance the cellular uptake and the cytotoxic effect against HER-2 positive cell line in comparison with non-targeted or Herceptin-targeted DTX-NPs. Thus, aptamer conjugation could improve the in vitro performance of Ecoflex NPs, which could be suggested as a potential DTX delivery system in HER-2 overexpressing cancers. In this regard, EIS method could play its role as a sensitive quantification method to obtain the optimized aptamer-conjugated NP systems.

Graphical abstract

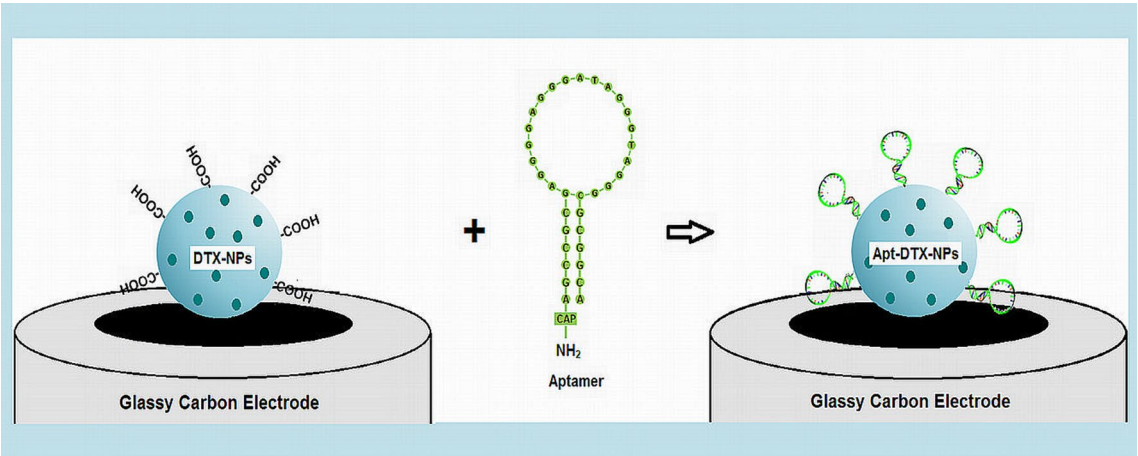

Keywords Aptamer · HER-2 receptor · Electrochemical impedance spectroscopy · Docetaxel · Ecoflex nanoparticles

Abbreviations

EIS	Electrochemical impedance spectroscopy
Apt	Aptamer

Extended author information available on the last page of the article

DTX	Docetaxel
ER	Estrogen
PR	Progesterone
EGFR	Epidermal growth factor receptor
AC	Alternating current
MTT	3-[4, 5-Dimethylthiazol-2-yl]-2,5-diphenyl tetrazolium bromide
EDC	N-(3-dimethylaminopropyl)-N′-ethylcarbodiimide hydrochloride
DMF	N,N-dimethyl formamide
NHS	N-hydroxysuccinimide
RPMI	Roswell Park Memorial Institute
FBS	Fetal bovine serum
NPs	Nanoparticles
DTX-NPs	Non-targeted docetaxel nanoparticles
Blank NPs	Docetaxel-free nanoparticles
Apt-NPs	Docetaxel-free aptamer-targeted nanoparticles
Hcp-NPs	Docetaxel-free Herceptin-targeted nanoparticles
Apt-DTX-NPs	Aptamer-targeted docetaxel nanoparticles
Hcp-DTX-NPs	Herceptin-targeted docetaxel nanoparticles
RhB	Rhodamine B

1 Introduction

Breast cancer could be taken into account as a heterogeneous disease, classified into luminal and basal epithelial phenotypes. In contrast to luminal type of breast cancer, the basal epithelial type is usually hormone-receptor and HER-2 receptor negative. The importance of investigating the presence of estrogen (ER), progesterone (PR), and HER-2/neu receptors is that they could be utilized as target for drug delivery systems [1, 2]. For instance, the presence of estrogen receptor indicates the possibility of performing endocrine therapy by administration of anti-estrogens such as tamoxifen, and in the case of HER-2 receptor positive cancers monoclonal antibodies against this receptor, such as trastuzumab, could be implemented [3].

HER-2 receptor is classified as a trans-membrane epidermal growth factor receptor (EGFR), which is overexpressed in several malignancies including breast, ovarian, and gastric cancers. The amplification of HER-2 receptor gene is accompanied by metastasis, poor prognosis, and reduced survival rate. Despite the advent of anti-HER-2 monoclonal antibodies, such as trastuzumab (1998, Genentech, USA) and pertuzumab (2012, Genentech, USA), due to lack of drug response or progression of drug resistance in patients, continuation of research for more HER2-targeted drugs is still a requisite [4].

Other drawbacks of antibodies are high cost and complex production procedure, limited shelf-life, and poor stability leading to denaturation. Regarding these factors, aptamers could provide satisfying alternatives, presenting notable advantages including high stability due to the nature of aptamer molecules, as well as ease of manufacturing and modification procedure [5, 6].

The concept of using aptamers emerged in 1990 and was built on the ability of short sequence nucleic acid molecules to form unique three-dimensional structures which could bind to a target molecule with high affinity and specificity. The in vitro selection of aptamers is performed via systemic evolution of ligands by exponential enrichment, known as SELEX. In this technique, various targets like proteins are incubated with a library of RNA/DNA sequences; afterward, following the isolation of complexes of protein and DNA, the process is repeated to achieve a sample of amplified sequence which demonstrates the best affinity toward the target protein [6].

The word aptamer is a combination of a Latin and a Greek expression: '*aptus*' which means 'to fit' and '*meros*' which means 'part' [7]. Aptamers are defined as short single-stranded RNA or DNA molecules, possessing specific three-dimensional sequence-dependent structures which are responsible for their ability to target-specific molecules [8]. The stability of aptamers is affected by their primary sequence, the size of molecule that is usually in the range of 25–90 bases, as well as the environmental circumstances, including heat or enzymatic cleavage. In order to avoid this cleavage or improve thermodynamic stability of aptamers, chemical modifications could be performed [9]. Aptamers are able to target both small molecules and macromolecules such as proteins. In the case of macromolecules, the affinity is usually higher due to the presence of abundant hydrogen-donor/acceptor areas, leading to dissociation constant values in the range of pico/nanomolar which is comparable to K_d of interaction between monoclonal antibodies and antigens. On the other hand, even minor structural differences in the target molecule could be differentiated by aptamer, leading to high specificity of aptamers as targeting agents [8, 10].

Electrochemical impedance spectroscopy (EIS) is one of the most reliable methods for characterization of electrochemical systems and could be applied to investigate the occurrence of microscopic processes. This technique is widely used in many fields of electrochemistry as one of the most sensitive tools applied to investigate the interfacial phenomena and effects of surface modification. Recently the use of EIS in bio-analysis techniques has shown a significant increment. One of the major advantages of this method, especially in surface modification of biological agents, is that instead of potential ramp, a small alternating current (AC) that is perturbation at open circuit potential is applied to the sample; therefore, the procedure is harmless and

would not destroy the sample when the analysis is going on [11–13].

One of the most noteworthy cytotoxic agents with clinically proven effects in prolonging the survival and improving the quality of life of patients suffering from breast cancer is docetaxel (DTX) (Taxotere®, Sanofi Aventis). The mechanism of its cytotoxic effect is preventing the formation of new cells by inhibition of the function of microtubules, and also induction of apoptosis in the existing cells by inhibition of the anti-apoptotic gene of Bcl2 that leads to expression of p2t and inhibition of the cell cycle [14–18]. However, healthy cells as well as tumor cells would undergo these mechanisms causing DTX-related adverse effects. The negative effects of treatment on patient's quality of life and health status could even lead to cessation or reduction of the administered dose and depriving the patient of the potential benefits of treatment [16]. Therefore, a lot of effort has been dedicated to produce targeted systems to directly deliver DTX to the tumor site and prevent non-specific drug distribution throughout the patients' body.

Polymeric nanoparticles are submicron-sized polymeric colloidal particles utilized as carriers for therapeutic agents via encapsulation of the drug cargo within their polymeric matrix or conjugation onto the surface. In this regard, biodegradable polymers have gained increasing attention for site-specific delivery of drugs [19]. Poly(butylene adipate-co-terephthalate) with the commercial name of Ecoflex® is a biodegradable synthetic aliphatic and aromatic biopolyester, which was initially introduced for application in agricultural films and food packaging. However, considering its characteristics including appropriate mechanical properties as well as lack of toxicity and environmental negative effects, this polymer is recently investigated for pharmaceutical applications [20].

Among various HER-2-specific aptamers that are investigated recently, Kim et al. [21] introduced a minimal version of an RNA aptamer, SE15-8, which could bind to HER-2 receptors with high affinity and specificity, while less difficulties were faced due to its smaller size. Tabasi et al. [22] implemented a single-stranded DNA version of the truncated SE15-8 aptamer, with addition of 5′-C6-amine and a 10-nucleic acid 5′ cap, to construct an aptasensor for detection of HER-2 receptor as an alternative to the currently applied methods including immunohistochemistry (IHC) and fluorescent in situ hybridization. High sensitivity and selectivity were reported, as well as a detection limit of 0.21 ng/mL, which is far below the clinical cutoff.

Therefore, the aim of current study was to investigate the use of a HER-2-specific aptamer, as a targeting ligand for HER-2 positive breast cancer using polymeric nanoparticles (NPs) of Ecoflex®. The attachment of this ligand to the NPs was optimized via electrochemical impedance spectroscopy method. The resulted aptamer-targeted docetaxel NPs (Apt-DTX-NPs) delivery system underwent in vitro evaluations in comparison with non-targeted nanoparticles to assess the effect of aptamer as the targeting agent.

2 Materials and methods

2.1 Materials

Docetaxel was provided by Cipla (India) and Ecoflex® (Mw = 100,000) by BASF Company (Germany). Pluronic F-127, 3-[4, 5-dimethylthiazol-2-yl]-2,5-diphenyl tetrazolium bromide (MTT), rhodamine B, N-(3-dimethylaminopropyl)-N′-ethylcarbodiimide hydrochloride (EDC), potassium ferricyanide, and potassium ferrocyanide were purchased from Sigma Company (US). PEG (Mw = 6000), acetonitrile, dichloromethane, N,N-dimethyl formamide (DMF) and N-hydroxysuccinimide (NHS) were from Merck Chemical Company (Germany). Roswell Park Memorial Institute (RPMI) medium, fetal bovine serum (FBS), and trypsin/EDTA were supplied by Biosera Europe (ZI du Bousquet, France), penicillin/streptomycin from Gibco (UK), Herceptin by Roche (Switzerland), and DNA aptamer with base sequence of (5′-AGCCGCGAGGGG AGGGATAGGGTAGGGCGCGGCT-3′) was custom-synthetized by Genfanavaran Co, Iran. BT-474 and MDA-468 cell lines were purchased from the Iranian Biological Resource Center.

2.2 Preparation of DTX-loaded Ecoflex® nanoparticles

DTX-loaded NPs were prepared by the electrospraying technique reported by Varshosaz et al. [23, 24]. Briefly, the organic phase, composed of DTX and Ecoflex® (in the ratio of 1:3) dissolved in dichloromethane: dimethyl formamide (with the ratio of 2.7:1), was dispersed in an aqueous solution containing 1% w/v of Pluronic F-127 using an electrospray at a voltage of 20 kV, 12 cm distance between electrodes, and feeding rate of 1 ml/hr. The result was an aqueous suspension of polymeric nanoparticles loaded with DTX.

2.3 Evaluation of aptamer conjugation to DTX-NPs by electrochemical impedance spectroscopy(EIS) method

Conjugation of aptamer molecules to DTX-NPs was performed by activation of carboxyl groups of Ecoflex® NPs by using EDC and NHS, followed by formation of amid bonds between these activated groups and the amine

groups of aptamer molecules. In order to compare the amount of aptamer molecules attached to the DTX-NPs in different conditions by EIS method, these reactions were performed on a working electrode. Addition of NPs to the working electrode would increase its charge transfer resistance (R_{ct}). Further increment of this value by attachment of aptamer molecules to the DTX-NPs placed on the surface of electrode was regarded as an index of the amount of aptamer molecules attached to the NPs.

Glassy carbon working electrode (2 mm diameter) was polished with alumina on polishing cloth and, then, placed in ethanol and sonicated using a micro-process controlled bench-top ultrasonic cleaner (power sonic 505, Hwashin technology, Korea).

Analyses were performed using potentiostat/galvanostat Autolab® instrument (Metrohm, Netherlands) in a conventional 3-electrode system: a glassy carbon working electrode, a platinum counter electrode, and an Ag/AgCl (saturated KCl) reference electrode. The working electrode was modified by addition of DTX-loaded NPs suspension onto the electrode surface, which would form a NPs-rich surface upon drying. The aptamer molecules were attached to the NPs through the following interactions. The modified electrode surface was washed to remove any loosely attached NPs that would affect the alterations in the resistance of working electrode; afterward, 2 µl of 400 mM solution of EDC and 100 mM solution of NHS were added to the surface of the electrode and maintained for a predetermined time period to activate –COOH functional groups present on the polymer chains constructing the NPs. Then, 2 µl of aptamer solution was added onto the surface of working electrode to form covalent amide bonds through the reaction of its amine functional groups and the activated COOH groups of Ecoflex®. Impedance was analyzed in 0.1 Hz-100 KHz frequency range, utilizing a 5 mV modulation voltage and redox probe composed of 0.3 M KCl solution containing 1:1 mixture of 10 mM $k_3[Fe(CN)_6]$: $k_4[Fe(CN)_6]$ [22].

2.4 Optimization of the process of aptamer conjugation to the NPs

In order to optimize the time of reaction between the polymer and EDC/NHS, as well as the reaction with aptamer molecules, and also the washing periods needed to remove the loosely bound aptamer molecules, a 3-factor, 3-level Box–Behnken design was used by Design Expert Software (version 7.1, US) and 17 different runs were done according to the proposed conditions by the software (Table 1). The difference between the impedance of the electrode in different steps of the procedure in each design was regarded as the response.

Table 1 Box–Behnken design for optimization of reaction parameters evaluated by electrochemical impedance spectroscopy and the related difference in diameter of semicircular portion (R_{ct}) of impedance plots in each run

Reaction time with EDC/NHS (min)	Reaction time with aptamer (min)	Washing time (sec)	Difference in R_{ct} (Ω)
20	120	105	569
55	30	30	222
20	75	30	790
20	30	105	353
55	120	30	389
55	75	105	497
55	75	105	503
90	120	105	186
55	75	105	445
20	75	180	745
55	75	105	458
55	75	105	425
55	120	180	410
90	30	105	136
55	30	180	212
90	75	180	282
90	75	30	271

2.5 Preparation of aptamer-targeted DTX-NPs in the optimized condition of conjugation

The aptamer targeting ligand was chemically conjugated to the DTX-NPs via an amide bond between the amine functional group on aptamer molecule and carboxylic acid group on Ecoflex® DTX-NPs. For this purpose according to the optimized condition found in the previous step, an aqueous suspension of DTX-NPs was incubated with 400 mM of EDC and 100 mM of NHS at room temperature for 20 min, which caused activation of the aforementioned –COOH groups. Afterward, activated NPs were incubated for 88 min with a 100 pM aqueous solution of aptamer as much as 2 weight% of the polymer concentration. The obtained aptamer-targeted DTX-NPs (Apt-DTX-NPs) were washed to remove unbound reagents [25, 26]. The same procedure was performed using Herceptin antibody instead of aptamer in order to construct Herceptin-targeted DTX-NPs (Hcp-DTX-NPs).

2.6 Particle size, particle size distribution, and zeta potential of NPs

The particle size, particle size distribution, and zeta potential of the NPs were determined by a laser light scattering particle size analyzer (Malvern instrument, UK). Samples were suspended in deionized water, and each measurement was performed in triplicate.

2.7 DTX loading efficiency measurement

The lyophilized powder of NPs was dispersed in an aqueous medium containing Tween® 80 to dissolve the free drug. Then, it was centrifuged (Eppendorf centrifuge 5430, Germany) at 14,000 rpm for 15 min and filtered through Amicon ultracentrifuge filter (cutoff 10,000 Da) (Millipore, Ireland) to separate the free drug from the NPs. The amount of free drug was determined by HPLC. Using the following equation, the entrapment efficiency was calculated:

$$\text{Entrapment efficiency } \% = \left(\frac{\text{total drug} - \text{free drug}}{\text{total drug}}\right) \times 100$$

2.8 DTX release profiles

In vitro release of DTX from the targeted NPs was studied in an aqueous medium of phosphate buffer (pH 7.4, 0.01 M) and 0.5 w/v% of Tween® 80. Briefly, an aqueous suspension of NPs was placed inside dialysis bag (cutoff 12,000 Da) in sufficient amount of release medium under gentle stirring at 37 ± 0.5 °C for 30 h to reach a final concentration of 1.3 µg/mL DTX when the drug cargo is thoroughly released. This concentration equals to15% of saturated solubility (9.8 ± 0.3 µg/ml) of DTX in the release medium, to keep the sink condition. Meanwhile, 100 µl of samples was withdrawn at predetermined time intervals and replaced with fresh medium to maintain the volume of release media. Samples were filtered using Amicon® filters before analyzing the DTX concentration by HPLC method.

2.9 HPLC analysis method

A UV detector at the wavelength of 230 nm and C-18 Column (Waters Spherisorb®, 5 µm ODS2 4.6 × 250 mm) were applied on HPLC system (Waters, USA). The mobile phase composed of acetonitrile–water (65:35, v/v) and the flow rate was set at 1 ml/min [27]. The standard curve was plotted in the range of 0.25–40 ng/ml, and peak area of DTX in each sample was analyzed using the line equation, considering inter-day and intra-day standard deviations.

2.10 In vitro cytotoxicity assay

BT-474 and MDA-468 were, respectively, the HER-2 positive and HER-2 negative cell lines [28]. The cells were maintained in RPMI 1640 culture medium supplemented with 10% FBS and 1% penicillin (100 IU/ml)-streptomycin (100 µg/ml). Incubation was done under 98% relative humidity and 5% CO_2. Cell suspensions containing 6×10^4 cell/ml of each cell line in 96-well plates were incubated for 24 h in the aforementioned condition. When the cells were attached, the wells were classified into groups that were treated with different samples including aptamer-targeted docetaxel NPs (Apt-DTX-NPs), Herceptin-targeted NPs (Hcp-DTX-NPs), non-targeted docetaxel NPs (DTX-NPs), free docetaxel and control samples including blank aptamer-targeted NPs (Apt-NPs), blank Herceptin-targeted NPs (Hcp-NPs) and blank non-targeted nanoparticles (NPs). Each sample was prepared as suspensions containing various contents of DTX; 10–100 ng/ml. Following 24 h of incubation, 20 µl of MTT solution (5 mg/ml) was added to each well and after another 3 h incubation period, the supernatant was replaced with DMSO to dissolve formazan crystals produce by alive cells. Finally, the cell survival in each treatment group was analyzed by measuring the absorbance at 570 nm using ELISA plate reader (Biotek instrument, USA).

The cytotoxicity assay was performed in triplicate and the cell survival in each treatment group was calculated by the following equation and the differences were evaluated statistically by ANOVA test followed by LSD post hoc test.

$$\text{Cell Survival\%} = \left(\frac{\text{absorbance of test group} - \text{absorbance of blank}}{\text{absorbance of control group} - \text{absorbance of blank}}\right) \times 100$$

2.11 Cellular uptake

Cellular uptake of the targeted and non-targeted NPs was investigated using rhodamine B (RhB) as a fluorescent probe which was entrapped instead of DTX in the NPs [29]. Using dialysis bag (cutoff 12,000 Da), free RhB was excluded and the release profile of RhB from NPs was studied in order to confirm that the fluorescence detected in the fluorescent microscope and flow cytometry studies was due to the uptake of NPs into the cells, not by the penetration of the released fluorochrome into the cells.

In order to perform the primary evaluations by microscopy, a sterilized 18-mm coverslip was pretreated with poly-L-lysine 0.1% solution and placed inside each well of a 12-well cell culture plate. Afterward, 450 µl samples of BT-474 and MDA-MB-468 cell suspensions with the concentration of 10^5 cell/ml were seeded in separate wells. After an initial incubation period to let the cells to attach to the coverslip, 50 µl of the samples including pure RhB, blank NPs (aptamer-targeted NPs that were not loaded with RhB), RhB-loaded NPs, and Herceptin-targeted or aptamer-targeted RhB-loaded NPs were added to each well. After a 2-h incubation period, coverslips were removed, gently washed with PBS, and placed on separate slides. The resulted slides were evaluated by fluorescent and light microscopy (Eclipse Ti-U; NIKON, Japan).

Also, in order to quantitatively compare the cellular uptake of aptamer-targeted NPs with non-targeted NPs, flow cytometric analysis was performed. The cells were seeded in 6-well plates and after 24 h of initial incubation different treatment samples were added and incubated for another 2 h.

Afterward, cells were collected, washed, and re-suspended in PBS for flow cytometry measurement using FACS Calibur (Becton Dickinson, USA).

3 Results and discussion

3.1 Choosing appropriate HER-2-specific ligand

In comparison with antibodies against tumor markers, aptamers have proven to be superior when implemented as targeting ligands, because aptamers have demonstrated higher selectivity and affinity, lower immunogenicity, simpler synthesis procedure, more rapid tissue penetration, and less toxic effects [30].

The aptamer used in the current study was a single-stranded DNA molecule with a sequence resembling the minimal version of SE15-8 RNA aptamer introduced by Kim et al. [21] confirmed its potential as a HER-2 targeting molecule with high affinity and specificity. In the current study, a single-stranded DNA molecule was constructed with the same sequence, but the uracil bases were replaced with thymidine, also an amine modification was performed to provide the opportunity of attachment to –COOH groups on the DTX-NPs constructed from Ecoflex®. The affinity of the resulted aptamer toward HER-2 receptor was investigated by Tabasi et al. [22]. In comparison with other HER-2 aptamers, main advantages that could be mentioned about the aptamer used in the current study include: first, regarding stability issues, DNA structure is not as vulnerable as RNA toward the environmental condition and presence of enzymes, such as RNases. Secondly, shorter sequence of this aptamer molecule which forms a simple hairpin structure could enhance its stability as well as simplicity and cost-effectiveness of manufacturing process [22].

3.2 Optimization of the reaction between NPs and aptamer molecules

The Nyquist plots obtained from EIS analysis of designed reaction conditions were analyzed to calculate the difference between charge transfer resistances (R_{ct}) in each design (Table 1). The resulted plots illustrated that alteration in reaction times led to difference in diameter of semicircle, which represents charge transfer resistance [31].

The amount of aptamer molecules attached to the NPs was evaluated using EIS. Analysis by EIS is an appropriate method for measurement of changes on electrode surface. Impedance spectra, shown as Nyquist diagram (Fig. 2), are composed of a semicircular portion at higher frequencies, and a linear portion at lower frequencies. The two portions are associated with charge-transfer-limited process and the diffusion process, respectively. The diameter of the semicircle corresponds with interfacial charge-transfer resistance. Presence of sample on the surface of electrode causes a hindrance effect on charge transfer process between $Fe(CN)^{3-/4-}$ and the electrode surface, which leads to increment of R_{ct} value [31]. In the current study, the difference between diameters of semicircular portion of Nyquist diagram, which indicates the difference between R_{ct} of the electrode after being treated with different samples, was used to judge the expected reaction. In other words, greater difference between the aforementioned values could be interpreted as more aptamer molecules attached to the NPs.

Implementation of EIS has attracted a great deal of interest in biosensor studies, since this method could offer the opportunity of investigating the different stages of fabrication of biosensor and attachment to the analytes, via monitoring the changes in electrical properties with minimum possible interruption in the biological interactions. Various studies have been performed on the aforementioned application of EIS as an appropriate measurement method for aptamer based biosensors, aptasensors. For instance, Chen et al. [32] reported an impedimetric aptasensor composed of aptamer molecules immobilized on gold NPs onto the electrode surface to quantify the amount of lysozyme. In their study, EIS was used to measure the increment of charge transfer resistance related to the increment of lysozyme concentration in the sample. In another study, Zhang [33] developed a novel high-performance electrochemical biosensor for detection of DNA hybridization in chronic myelogenous leukemia (CML). In this genosensor, EIS was implemented to monitor R_{ct}. Also for cancer diagnosis purposes, EIS could provide a sensitive, selective, and at the same time economical device. Some examples include the aforementioned study by Tabasi et al. [22] and also an RNA/peptide dual aptamer probe investigated by Min et al. [34] for diagnosis of both PSMA positive and negative prostate cancer. This probe included an aptamer-modified electrode which demonstrated an increased R_{ct} when exposed to target cancer cells, indicating a direct interaction between aptamer and these cells.

Aptamer molecules are also under investigation as appropriate alternatives for other targeting ligands including monoclonal antibodies, due to their remarkable advantages including simplicity of chemical synthesis and storage, versatility, possibility of modification, and stability [32]. But there is lack of sensitive measurement method to quantify small amounts of aptamer molecules attached to the delivery system without destructing the aptamer molecule. In some of the previous studies on aptamer-targeted delivery systems, the attachment of aptamer molecules to the drug-loaded NPs was not quantified [25, 26], and in some cases UV-spectrophotometric method was used [35], which is not cost-effective due to high amount of aptamer needed to be detected. Therefore, EIS analysis could provide a suitable

method to offer the opportunity of quantitatively investigating the attachment of NPs to aptamer molecule, due to its sufficient sensitivity. Thus, the parameters that are effective on the reaction between aptamer and NPs (Table 1) could be optimized.

Figure 1 shows the effect of the studied variables on the impedance difference.

In the optimization process, 17 conjugation conditions were designed by the Design Expert Software. In each design, the diameter of the semicircular part of the Nyquist diagram was obtained to calculate the difference between R_{ct} value, before and after addition of the aptamer molecules to the EDC/NHS-activated NPs. This R_{ct} difference was interpreted as the amount of aptamer molecules attached to the NPs surface; thus, it was considered as the response data that were entered for each design. The results of evaluation by Design Expert software revealed that, although a minimum reaction time of about 20 min is needed for EDC/NHS-activation, increment of this reaction time would negatively affect the response (Fig. 1). This minimum reaction time was obtained in our pilot studies. On the other hand, increment of reaction time between the activated NPs and aptamer molecules up to 90 min increased the regarded response, and further increment of this reaction time would negatively affect the response (Fig. 1). Washing period, which could simulate the detachment or denaturation of aptamer molecules when the drug delivery system enters aqueous environments, did not have any significant effect on the response (Fig. 1).

An RCRW circuit was used to fit the experimental data, afterward, using Design Expert Software. The effect of reaction time needed for activation of –COOH groups, the reaction time needed for attachment of aptamer molecules to the activated DTX-NPs, and washing periods were analyzed and the optimum condition for the conjugation of aptamer to the NPs was suggested to be 20 min, 88.76 min, and 30 s, for aforementioned variables, respectively.

Then, the optimum situation proposed by the software was performed and analyzed by EIS and the Nyquist plots were obtained before and after the addition of the aptamer molecules to the EDC/NHS-activated DTX-Nps and the difference between R_{ct} values of these two plots was calculated as the experimental data (Fig. 2); then, it was compared to the predicted data to check the accuracy of the predicted results versus the obtained ones. The predicted difference by the software for the optimum situation was 780.43 Ω while its actual value obtained 759 Ω which showed about 2% of error in predicting the variables.

3.3 Physicochemical properties of the targeted and non-targeted NPs

Regarding particle size distribution, entrapment efficiency, and release efficiency, DTX-NPs resembled Apt-DTX-NPs (Table 2), therefore, addition of the aptamer molecule did not have any significant alteration on these characteristics, while the differences between particle size and zeta potential were significant.

The Ecoflex NPs demonstrated high entrapment efficiency in comparison with other polymeric NPs investigated in previous studies. For example, previously studied DTX-loaded polymeric nanoparticles of PLA, PLGA, PLA-PCL, and PLGA-PCL demonstrated entrapment efficiencies in range of 19.7–47.2%, while the Ecoflex DTX-NPs fabricated

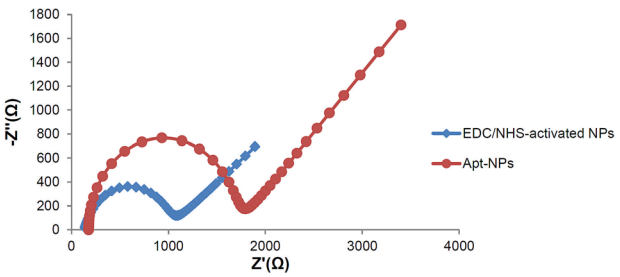

Fig. 2 Nyquist diagrams related to the optimum condition of conjugation the aptamer to NPs. The differences between the semicircular portions in Nyquist plots for EDC/NHS-activated DTX-NPs and Apt-DTX-NPs

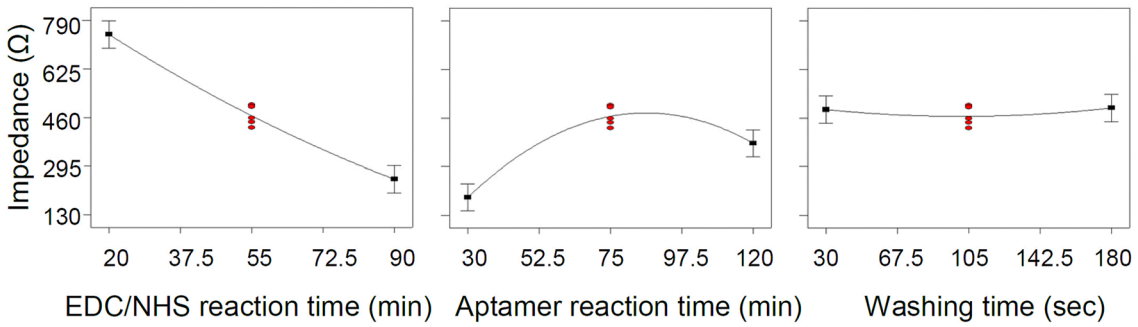

Fig. 1 Evaluation of the effect of each parameter on the predetermined response using Box–Behnken design

Table 2 Comparison of physicochemical properties targeted and non-targeted nanoparticles of Ecoflex loaded with docetaxel (PDI = polydispersity index, RE_{30}%= release efficiency over 30 h of release test)

Formulation	Particle size (nm)	PDI	Zeta potential (mV)	RE_{30} (%)	Entrapment efficiency (%)
NPs	202.4 ± 8.3	0.29 ± 0.01	− 17.6 ± 0.4	47.1 ± 1.6	82.0 ± 8.5
Apt-NPs	274.7 ± 46.1	0.44 ± 0.02	− 9.9 ± 0.19	47.7 ± 1.9	75.3 ± 1.5

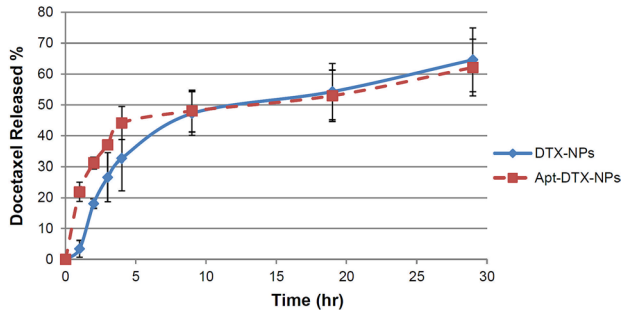

Fig. 3 Release profiles of DTX from DTX-NPs in comparison with Apt-DTX-NPs

in the current study had significantly higher entrapment efficiency (82.0 ± 8.5) [36].

3.3.1 DTX release profile from Apt-DTX-NPs

Drug release profile from Apt-targeted NPs in comparison with non-targeted NPs is demonstrated in Fig. 3. Release efficiency percent of DTX in Apt-DTX-NPs and non-targeted DTX-NPs were 47.69 ± 1.64% and 47.09 ± 1.93%, respectively, which shows no significant difference ($p < 0.05$) in drug release rate after modification of the NPs surface with aptamer.

According to the DTX release profiles from DTX-NPs and Apt-DTX-NPs, it could be concluded that drug release from the targeted NPs was not affected significantly, by the attachment of aptamer molecules on the surface of NPs.

3.4 In vitro cytotoxicity assay

BT-474 and MDA-MB-468 cells were treated with DTX-NP suspension, Herceptin-targeted DTX-NP, aptamer-targeted DTX-NPs, free drug, and control samples of DTX-free NPs and DMSO. The survival percent of the cells in each group are presented in Fig. 4.

In vitro cytotoxicity, investigated by MTT assay, revealed a significant reduction in cell survival in both cell lines, when treated with DTX-NPs compared to free DTX, at concentrations equal to 30–50 ng/mL of DTX (Fig. 4). Besides, treatment of BT-474 cells (HER-2 positive breast cancer cell line) with targeted DTX-NPs, caused a significantly lower

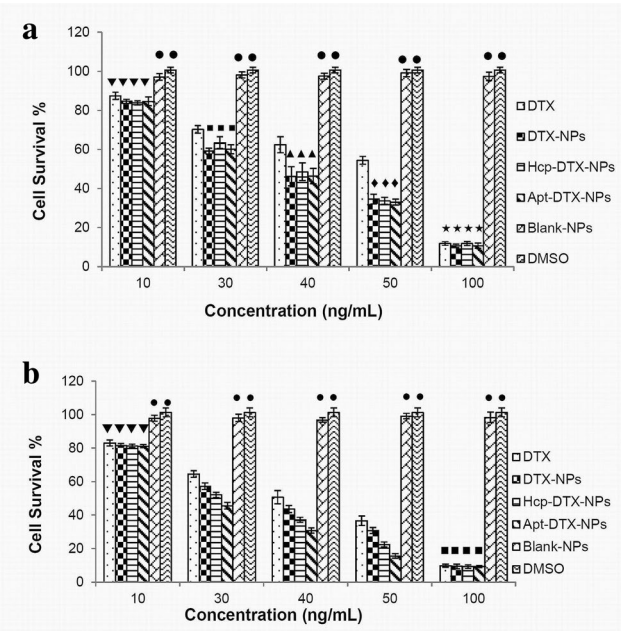

Fig. 4 Survival percent of **a** MDA-MB-468 cells and **b** BT-474 cells treated with DTX-NPs, Apt-DTX-NPs, Hcp-DTX-NPs, and free drug with different concentrations in the range of 10–100 ng/mL; and also control samples including blank NPs (non-targeted, Apt-targeted, and Hcp-targeted NPs that are DTX free), and DMSO with the maximum concentration used in treatment groups. Diagrams demonstrated with same symbol did not have significant difference ($p > 0.05$) with each other

cell survival, in comparison with the non-targeted NPs, while the difference between these two treatments was not significant in MDA-MB-468 cells (HER-2 negative breast cancer cell line) (Fig. 4). It is noteworthy that cell survival observed in BT-474 cells treated with Apt-DTX-NPs was significantly ($p < 0.05$) lower than those treated with Hcp-DTX-NPs (Fig. 4). In order to confirm lack of toxicity in delivery system, blank NPs were used as control which did not show any significant cytotoxic effect, even at the highest concentration used to treat both cell lines (Fig. 4); hence, the safety of the suggested delivery system could be confirmed. Therefore, with regard to the results of MTT assay, the designed NPs could enhance the cytotoxic effect of DTX on breast cancer cell lines by its own (Fig. 4). Moreover, on receptor positive cells, this effect is amplified by addition

of targeting ligands and eventually, in the case of the targeting ligand, aptamer seems to perform more efficiently than Herceptin (Fig. 4). Increment of cellular uptake would explain the enhanced cytotoxic effect of DTX in the targeted delivery systems (Fig. 5).

3.5 Cellular uptake

Fluorescence micrographs of BT-474 and MDA-MB-468 cells, treated with free RhB and RhB-loaded NPs, are presented in Fig. 5. Detection of fluorescence in cells confirmed that the sample has been up-taken by the cells because the cells were washed after being exposed to samples. Since free RhB had not entered the cells, no fluorescence was observed in fluorescence micrographs. In contrast, the RhB-loaded NPs were successfully up-taken by the cells; this could verify the ability of this nanoparticulate delivery system to enter the cancer cells.

Quantitative analysis performed by flow cytometry offered the possibility of comparing the cellular uptake of blank NPs, free RhB, RhB-NPs, Apt-RhB-NPs, and Hcp-RhB-NPs in HER-2 positive and HER-2 negative cell lines. The obtained results are presented in Figs. 5 and 6, illustrating higher cellular uptake of entrapped RhB in

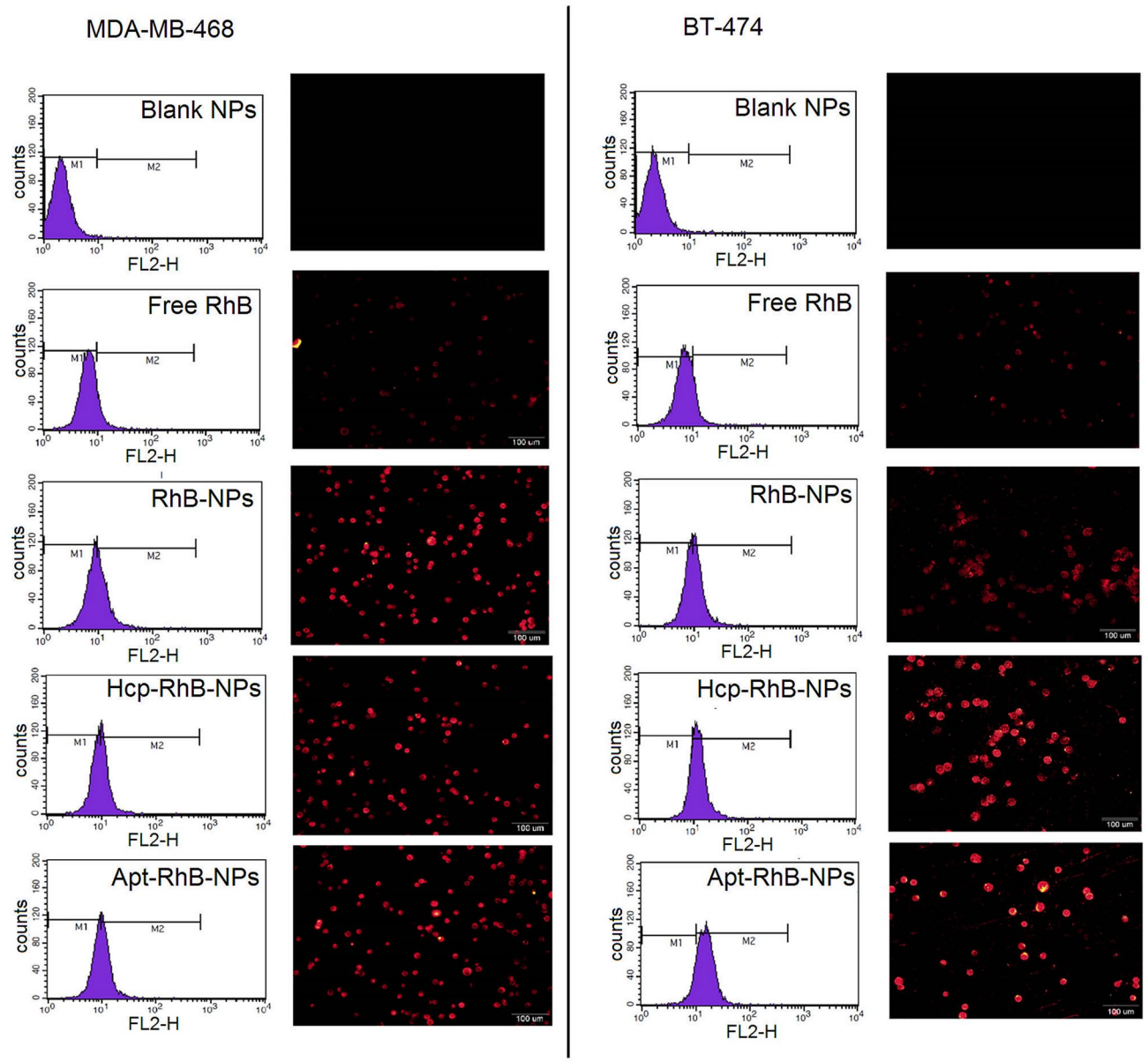

Fig. 5 Fluorescence micrographs and flow cytometry diagrams indicating the count of BT-474 and MDA-MB-468 cells in which fluorescence was detected after treatment with blank NPs, free RhB, RhB-NPs, Apt-RhB-NPs, and Hcp-RhB-NPs

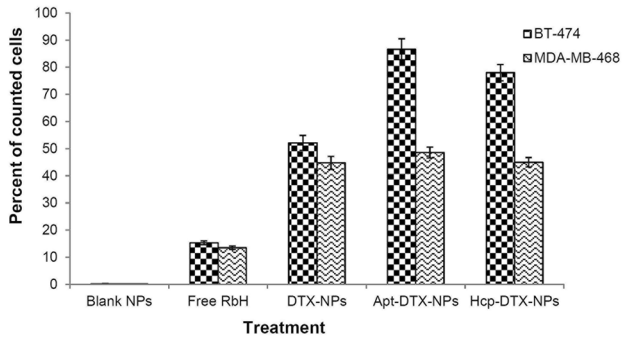

Fig. 6 Percent of BT-474 and MDA-MB-468 cells counted as fluorescence event in flow cytometry analysis, after treatment with blank NPs, free RhB, RhB-NPs, Apt-RhB-NPs, and Hcp-RhB-NPs

comparison with free RhB, and also higher cellular uptake of aptamer or HER-2-targeted NPs in receptor positive cells compared with non-targeted ones. Results demonstrated significantly higher cellular uptake of entrapped RhB in comparison with free RhB, and also higher cellular uptake of targeted NPs in receptor positive cells compared with non-targeted NPs. When aptamer was used as the targeting ligand, the NPs were up-taken slightly more than those targeted with Herceptin. These results would justify the results of in vitro cytotoxicity assay (Fig. 4).

4 Conclusions

Aptamers are suggested as sensitive, selective, stable, and cost-effective, substitutes for monoclonal antibodies in targeted drug delivery. In this investigation, EIS is proposed as a sensitive and reliable technique to evaluate the amount of aptamer molecules attached as a targeting ligand to the surface of drug delivery system. The HER-2-specific aptamer molecule investigated in current study demonstrated satisfying performance in comparison with free drug in vitro. Regarding the results obtained, the electrochemical impedance spectroscopy showed to be a valuable technique to evaluate the conjugation of aptamer to polymeric nanoparticles and the in vitro performance of Apt-DTX-NPs suggests this targeted delivery system has promising potential to be utilized in delivery of anticancer agents to HER-2 positive tumor site.

Acknowledgements The authors appreciate financial support of Isfahan University of Medical Sciences.

Compliance with ethical standards

Conflict of interest The authors declare no conflicts of interest.

References

1. Anderson WF, Matsuno R (2006) Breast cancer heterogeneity: a mixture of at least 2 main types. J Natl Cancer Inst 98:948–951
2. Basu S, Chen W, Tchou J, Mavi A, Cermik T, Czerniecki B et al (2008) Comparison of triple-negative and estrogen receptor-positive/progesterone receptor-positive/HER2-negative breast carcinoma using quantitative fluorine-18 fluorodeoxyglucose/positron emission tomography imaging parameters. Cancer 112:995–1000
3. Bauer KR, Brown M, Cress RD, Parise CA, Caggiano V (2007) Descriptive analysis of estrogen receptor (ER)-negative, progesterone receptor (PR)-negative, and HER2-negative invasive breast cancer, the so-called triple-negative phenotype. Cancer 109:1721–1728
4. Shen G, Yu H, Bian G, Gao M, Liu L, Cheng M et al (2013) Genistein inhibits the proliferation of human HER2-positive cancer cells by downregulating HER2 receptor. Functional Foods in Health Disease 3:291–299
5. O'Sullivan CK (2002) Aptasensors—the future of biosensing. Anal Bioanal Chem 372:44–48
6. Murphy MB, Fuller ST, Richardson PM, Doyle SA (2003) An improved method for the in vitro evolution of aptamers and applications in protein detection and purification. Nucleic Acids Res 31:110
7. Ellington AD, Szostak JW (1990) In vitro selection of RNA molecules that bind specific ligands. Nature 346:818–822
8. Peyrin E (2009) Nucleic acid aptamer molecular recognition principles and application in liquid chromatography and capillary electrophoresis. J Sep Sci 32:1531–1536
9. Wang RE, Wu H, Niu Y, Cai J (2011) Improving the stability of aptamers by chemical modification. Curr Med Chem 18:4126–4138
10. Mascini M, Palchetti I, Tombelli S (2012) Nucleic acid and peptide aptamers: fundamentals and bioanalytical aspects. Angew Chem Int Ed Engl 51:1316–1332
11. Ates M (2011) Review study of electrochemical impedance spectroscopy and equivalent electrical circuits of conducting polymers on carbon surfaces. Prog Org Coat 71:1–10
12. Schwake A, Geuking H, Cammann K (1998) Application of a new graphical fitting approach for data analysis in electrochemical impedance spectroscopy. Electroanalysis 10:1026–1029
13. Gebala M, Schuhmann W (2010) Controlled orientation of DNA in a binary SAM as a key for the successful determination of DNA hybridization by means of electrochemical impedance spectroscopy. Chem Phy Chem 11:2887–2895
14. Shelley M, Harrison C, Coles B, Staffurth J, Wilt TJ, Mason MD (2006) Chemotherapy for hormone-refractory prostate cancer. Cochrane Database Syst Rev 4:1–70
15. van Poppel H (2005) Recent docetaxel studies establish a new standard of care in hormone refractory prostate cancer. Can J Urol 12:81–85
16. Baker J, Ajani J, Scotte F, Winther D, Martin M, Aapro MS et al (2009) Docetaxel-related side effects and their management. Eur J Oncol Nurs 13:49–59
17. Perez EA (2009) Microtubule inhibitors: Differentiating tubulin-inhibiting agents based on mechanisms of action, clinical activity, and resistance. Mol Cancer Ther 8:2086–2095
18. Youm I, Yang XY, Murowchick JB, Youan BC (2011) Encapsulation of docetaxel in oily core polyester nanocapsules intended for breast cancer therapy. Nanoscale Res Lett 6:30
19. Mahapatro A, Singh DK Biodegradable nanoparticles are excellent vehicle for site directed in-vivo delivery of drugs and vaccines. J Nanobiotechnology 9: 55–66
20. Varshosaz J, Riahi S, Ghassami E, Jahanian-Najafabadi A (2017) Transferrin-targeted poly(butylene adipate)/terephthalate

nanoparticles for targeted delivery of 5-fluorouracil in HT29 colorectal cancer cell line. J Bioact Compat Pol 32:503–527
21. Kim MY, Jeong S (2011) In vitro Selection of RNA aptamer and specific targeting of ErbB2 in breast cancer cells. Nucleic Acid Ther 21:73–178
22. Tabasi A, Noorbakhsh A, Sharifi E (2017) Reduced graphene oxide-chitosan-aptamer interface as new platform for ultrasensitive detection of human epidermal growth factor receptor 2. Biosens Bioelectron 95:117–123
23. Varshosaz J, Ghassami E, Noorbakhsh A, Jahanian-Najafabadi A, Minayian M, Behzadi R (2018) Poly (butylene adipate-co-butylene terephthalate) nanoparticles prepared by electrospraying technique for docetaxel delivery in ovarian cancer induced mice. Drug Dev Ind Pharm 44:1012–1022
24. Ghassami E, Varshosaz J, Jahanian-Najafabadi A, Minaiyan M, Rajabi P, Hayati E (2018) Pharmacokinetics and in vitro/in vivo antitumor efficacy of aptamer-targeted Ecoflex® nanoparticles for docetaxel delivery in ovarian cancer. Int J Nanomed 13:493–504
25. Farokhzad OC, Cheng J, Teply BA, Sherifi I, Jon S, Kantoff PW et al (2006) Targeted nanoparticle-aptamer bioconjugates for cancer chemotherapy in vivo. PNAS 103:6315–6320
26. Farokhzad OC, Jon S, Khademhosseini A, Tran TNT, LaVan DA, Langer R (2004) Nanoparticle-aptamer bioconjugates: a new approach for targeting prostate cancer cells. Cancer Res 64:7668–7672
27. Varshosaz J, Taymouri S, Hassanzadeh F, Haghjooy Javanmard S, Rostami M (2015) Folated synperonic-cholesteryl hemisuccinate polymeric micelles for the targeted delivery of docetaxel in melanoma. Biomed Res Int 1–17
28. Anido J, Matar P, Albanell J, Guzma´n M, Rojo F, Arribas J et al (2003) ZD1839 a specific epidermal growth factor receptor (egfr) tyrosine kinase inhibitor induces the formation of inactive egfr/her2 and egfr/her3 heterodimers and prevents heregulin signaling in her2-overexpressing breast cancer cells. Clin Cancer Res 9:1274–1283
29. Xu Z, Chen L, Gu W, Gao Y, Lin L, Zhang Z et al (2009) The performance of docetaxel-loaded solid lipid nanoparticles targeted to hepatocellular carcinoma. Biomaterials 30:226–232
30. Hu Z, Tan J, Lai Z, Zheng R, Zhong J, Wang Y et al (2017) aptamer combined with fluorescent silica nanoparticles for detection of hepatoma cells. Nanoscale Res Lett 12:96
31. Teymourian H, Salimi A, Firoozia S (2013) A high performance electrochemical biosensing platform for glucose detection and ige aptasensing based on Fe3O4/reduced graphene oxide nanocomposite. Electroanalysis 25:1–10
32. Chen Z, Li L, Zhao H, Guo L, Mu X (2011) Electrochemical impedance spectroscopy detection of lysozyme based on electrodeposited gold nanoparticles. Talanta 83:1501–1506
33. Zhang WJ (2016) Application of Fe3O4 nanoparticles functionalized carbon nanotubes for electrochemical sensing of DNA hybridization. Appl Electrochem 46:559
34. Min K, Song KM, Cho M, Chun YS, Shim YB et al (2010) Simultaneous electrochemical detection of both PSMA (+) and PSMA(-) prostate cancer cells using an RNA/peptide dual-aptamer probe. Chem Commun 46:5566–5568
35. Yu C, Hu Y, Duan J, Yuan W, Wang C, Xu H et al (2011) Novel aptamer-nanoparticle bioconjugates enhances delivery of anticancer drug to MUC1-positive cancer cells in vitro. PLOS One 6:1–8
36. Sanna V, Roggio AM, Posadino AM, Cossu A, Marceddu S, Mariani A et al (2011) Novel docetaxel-loaded nanoparticles based on poly(lactide-co-caprolactone) and poly(lactideco-glycolide-co-caprolactone) for prostate cancer treatment: formulation, characterization, and cytotoxicity studies. Nanoscale Res Lett 6:260

Affiliations

Jaleh Varshosaz[1,5] · Erfaneh Ghassami[1] · Abdollah Noorbakhsh[2] · Ali Jahanian-Najafabadi[3] · Mohsen Minayian[4]

✉ Jaleh Varshosaz
varshosaz@pharm.mui.ac.ir

Erfaneh Ghassami
ghassami@pharm.mui.ac.ir

Abdollah Noorbakhsh
a.noorbakhsrezaei@ast.ui.ac.ir

Ali Jahanian-Najafabadi
jahanian@pharm.mui.ac.ir

Mohsen Minayian
minayian@pharm.mui.ac.ir

[1] Department of Pharmaceutics, School of Pharmacy and Novel Drug Delivery Systems Research Centre, Isfahan University of Medical Sciences, Isfahan, Iran

[2] Department of Nanotechnology Engineering, Faculty of Advanced Sciences and Technology, University of Isfahan, Isfahan, Iran

[3] Department of Pharmaceutical Biotechnology, School of Pharmacy, Isfahan University of Medical Sciences, Isfahan, Iran

[4] Department of Pharmacology, School of Pharmacy, Isfahan University of Medical Sciences, Isfahan, Iran

[5] Department of Pharmaceutics, Faculty of Pharmacy and Novel Drug Delivery Systems Research Centre, Isfahan University of Medical Sciences, PO Box 81745-359, Isfahan, Iran